

# Adaptive Spatial Compounding for Needle Visualization

B. Zhuang, K. Dickie, and L. Pelissier

**Abstract**— In this paper, we have proposed an adaptive tensor-analysis based spatial compounding method to enhance the needle visualization. *In-vitro* study has proved that the needle CNR has been improved from 0.78 to 4.58 without introducing significant artifacts. Meanwhile, no manual adjustments are needed during the procedure since the proposed method can enhance the needle with a big range of insertion angles under the same configuration. We believe the proposed method could be useful in the real-time guidance of needle insertion.

**Index Terms**—Spatial Compounding, Tensor-based analysis, needle enhancement

## I. INTRODUCTION

Ultrasonography has been increasingly used for the guidance of needle insertion such as nerve blocks, vascular access, biopsy, and therapy procedures [1, 2]. However, visualizing the needles inside the ultrasound image could be challenging due to the small needle footprint and the tissue/speckle pattern surrounding the needles. Failures in localizing the needle position have been documented even with experienced operators [3]. These failures could result in unnecessary tissue damages and increased patient discomfort. Therefore, substantial efforts have been put in the past to enhance the needle localization. One straightforward way would be having mechanical guides to fix the needle position/angle relative to the ultrasound probe [4]. In this case, the trajectory of the needle path in the body can be predicted and the needle will always be inside the ultrasound image plane. The problem for this approach is it requires complete reinsertion of the needle when the injection path is changed, and the actual needle tip position is unknown [5]. Echo-enhanced needles have also been proposed to improve the needle visualization [6]. These types of needles have coats that have large acoustic impedance difference compared with surrounding tissue, which increases the sound reflection. Although it has potential, some previous study has shown that there was no difference in procedure performance time between echo-enhanced and regular needles [7]. Increased needle cost could also limit its applications.

Recently, beam steering has been employed in many commercially available ultrasound systems to enhance the needle visualization [8]. It can effectively enhance the ultrasound beam reflection when the needle is close-to perpendicular to the ultrasound beam. To achieve the best enhancement, users need to adjust the beam-steering direction depending on which side of the probe the needle will be inserted in, and its insertion angle relative to the probe surface. When the needle path is adjusted during the procedure, which is common in nerve block access cases, the beam-steering angle has to be changed accordingly, which increases the operation complexity. Meanwhile, only needle should be enhanced while other tissue structure should not be highlighted indicating the needs for adaptive high performance filters. In this paper, we propose a new method that can enhance the needle without manual adjustments. It utilizes the adaptive spatial compounding technique with a tensor-based image processing algorithm [9]. Using spatial compounding to enhance the needle visualization is not new [10]. However, the traditional way of spatial

compounding can only enhance the needle visualization to a certain extent to avoid merging the low-quality images with large steering angles. Thus, the needles can only be enhanced when it's inserted with a small angle relative to the probe surface. Straightforward averaging also degrades the needle strength. To overcome this limitation, we propose to use multiple frames with a big variety of steering angles to enhance the needle regardless of its insertion direction. This minimizes the user adjustment during the procedure. Special adaptive processing algorithm is also proposed on each steered frame to isolate the possible needles while avoiding artifacts.

The paper is structured as follows: Section II presents the system parameters configuration for the proposed adaptive spatial compounding method, followed by the back-end processing algorithm including a Tensor-analysis based needle enhancement method. Phantom and *in-vitro* results are presented in Section III. Finally, Sections IV and V present discussions and conclusions.

## II. METHODS

### A. System configuration for adaptive spatial compounding

Figure 1 shows one possible system configuration of the proposed adaptive spatial compounding method. The blue trapezoid shapes represent regular B-mode frames undergoing traditional spatial compound processing, and the red trapezoid images represent special frames to enhance the needle. The number of needle-enhancement (NE) frames is not fixed. In this example, six NE frames with steering angles of -45, -30, -15, 15, 30, and 45 degrees are used. For probes with high-steering capability, the NE frame could have a steering angle up to 60 degree to detect needles with deep insertion angles. The goal of the NE frames is to enhance the needle while not degrade the compound image quality. The ideal processed result for NE frames would be images with needle only or completely black. Thus, NE frames can have low line density, e.g. 64 scan lines, to speed up the image acquisition. The transmit frequency for the NE frames is set also low, e.g. 5 MHz, to produce strong echo due to less attenuation. No tissue harmonic imaging is used in NE frames since it might cancel out the needle echo [2].

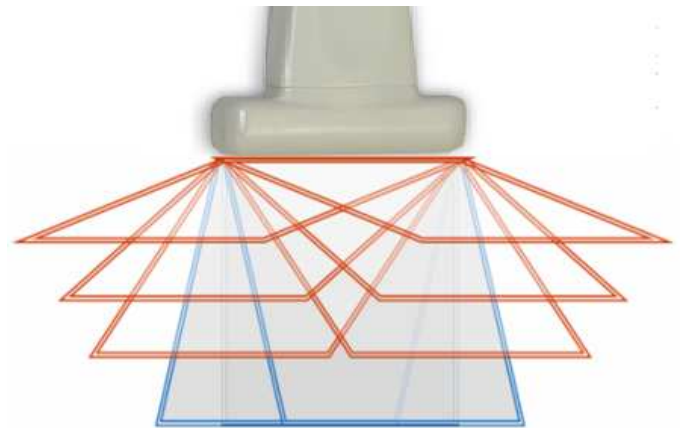


Fig. 1 An example of the proposed adaptive spatial compounding method. The blue trapezoid images show the frames using traditional spatial compounding method and the red trapezoid images show the special frames to enhance the needle.

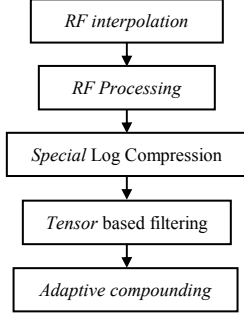


Fig. 2 The flow chart of the backend processing chain for NE frames.

### B. Back-end processing for NE frames

All the NE frames will go through a special back-end processing path to make sure only the needle is enhanced. The detail steps are listed in Fig. 2. Firstly, the RF data are interpolated twice or four times laterally due to the low quality needle image generated from 64 lines. The result data will be demodulated and envelope detected to generate the B-mode data. A special Log-compression will be applied on the envelope-detected data to remove the noise, and compress the result into a designed range, e.g. 8-bit. Different from regular log-compression, low-echo data will all be removed in the NE frames. For example, assuming the envelope-detected data has a range of 96-dB. The data from 0 to 50 dB are set to zero, and only the data above the 50 dB will be compressed into the 0-255 output range. This processing generates an image that only has needles, although the needle echo could be very weak. To enhance the weak needle echo, a tensor-analysis based adaptive filtering method is employed. It could also remove the remaining speckle noise in the needle image. The detail is introduced in the next section. The filtered needle image is finally merged back to other compounding images. Since the NE frames have different frequency, different gain factors should be applied on these frames to avoid the line artifact in the boundaries of the compounded image.

### C. Tensor based image filtering

Local tensor analysis is commonly used in image and signal processing fields to analyze the local structure of the signal [11]. The basic format of a 2D tensor,  $T$ , can be represented as follows:

$$T = \lambda_1 e_1 e_1^T + \lambda_2 e_2 e_2^T \quad (1)$$

where  $\lambda_1$  and  $\lambda_2$  are the major and minor Eigen values of the tensor, respectively.  $e_1$  and  $e_2$  are the corresponding Eigen vectors. In our applications, the part of the image that has needle will have a dominant  $\lambda_1$  compared with  $\lambda_2$ . While in the noise region, the  $\lambda_1$  and  $\lambda_2$  will be comparable and small. Therefore, once we have estimated the Eigen values for each local pixel, we can re-arrange these values, e.g. make large  $\lambda_1$  even larger and reduce the corresponding  $\lambda_2$ , to enhance the needle strength while making the needle boundary sharp. For the speckle-noise region, we can just reduce both  $\lambda_1$  and  $\lambda_2$  further to smooth it out.

Many different methods have been proposed to estimate the local tensor [12]. One of the common approaches is to use a set of polar separable quadrature directional filters [11]. In this case, the tensor can be calculated using the following equation:

$$T = \sum_{k=1}^4 |q_k| M_k \quad (2)$$

where  $q_k$  is the filter outputs from directional filters and  $M$  is the dual tensor basis corresponding to the tensor basis  $N_k = n_k n_k^T$ .

$$\begin{aligned} n_1 &= (1 \ 0)^T & n_3 &= (0 \ 1)^T \\ n_2 &= \left(\frac{1}{\sqrt{2}} \ \frac{1}{\sqrt{2}}\right)^T & n_4 &= \left(-\frac{1}{\sqrt{2}} \ \frac{1}{\sqrt{2}}\right)^T \end{aligned} \quad (3)$$

$n_k, k = 1, 2, 3, 4$  are the four directional unit vectors corresponding to the four directional filters with 0, 45, 90, and 135 degrees, respectively. The calculated dual tensor basis following the method introduced in [12] are:

$$\begin{aligned} M_1 &= \begin{bmatrix} 0.75 & 0 \\ 0 & -0.25 \end{bmatrix}; & M_2 &= \begin{bmatrix} 0.25 & 0.5 \\ 0.5 & 0.25 \end{bmatrix}; \\ M_3 &= \begin{bmatrix} -0.25 & 0 \\ 0 & 0.75 \end{bmatrix}; & M_4 &= \begin{bmatrix} 0.25 & -0.5 \\ -0.5 & 0.25 \end{bmatrix}. \end{aligned} \quad (4)$$

Once the tensor for every local pixel has been estimated, the major and minor Eigen values can be calculated through Eigen value decomposition. The calculated  $\lambda_1$  and  $\lambda_2$  will go through an Eigen-value remapping stage to enhance the needle while removing the noise using the following equations:

$$\gamma_1 = m \times \frac{\left(\frac{\lambda_1}{\|T\|}\right)^2}{\left(\frac{\lambda_1}{\|T\|}\right)^2 + \left(\frac{s}{\|T\|}\right)^2}, \quad \gamma_2 = \frac{\left(\frac{\lambda_2}{2\lambda_1}\right)^2}{\left(\frac{\lambda_2}{2\lambda_1}\right)^2 + \left(0.5 - \frac{\lambda_2}{2\lambda_1}\right)^2} \quad (5)$$

where  $m$  is the enhancement factor that can improve the needle strength,  $s$  is the smooth factor that will make the small Eigen values smaller,  $\|T\|$  is the maximum Eigen values throughout the image.

$\gamma_1$  and  $\gamma_2$  are the adjusted new Eigen values. To enhance the strength of the needle, we set  $m$  equal to 8 and  $s$  to 3.5. The new tensor,  $C$ , is created using the old Eigen-vectors,  $e_1, e_2$ , and the transformed Eigen-values  $\gamma_1$  and  $\gamma_2$  following the Equation (1). Once the new tensor is generated, the last step would be modifying the NE frames based on the new tensor. One direct way would be creating four directional high-pass filters following the same directions as the directional unit vectors. These high-pass filters will be convolved with the NE frames and generate four different values for each pixel in NE frames. The final value of any pixel is a weighted combination of four filtered values in the same location. The weight,  $w_k$ , is calculated by the dot multiply between the new tensor with its corresponding dual tensor basis as shown in equation (6).

$$w_k = c_{1,1} M_k(1,1) + c_{1,2} M_k(1,2) + c_{2,1} M_k(2,1) + c_{2,2} M_k(2,2) \quad k=1,2,3,4 \quad (6)$$

### D. Algorithm verification design

We will perform both phantom and *in-vitro* study to evaluate the proposed algorithm. Six NE frames with steering angles of -45, -30, -15, 15, 30, and 45 degrees are employed. A 19-gauge nerve block needle manufactured by Ultrasonix Med. Corp., Richmond, BC, is used in the study. Blue phantom, Redmond, WA, is used for phantom study and normal chicken breast is used for *in-vitro* study. We have implemented our algorithm in a SonixTablet ultrasound system, Richmond, BC, Canada. Since the proposed method has high computation and data requirements, all the software processing is optimized with SSE intrinsic to achieve real-time performance. As a comparison, the proposed adaptive compounding method will be compared with regular spatial compounding (with -10, 0, 10 degrees of steering). Our goal is to enhance the needle while limiting the manual adjustments during the procedure. Therefore, we will insert

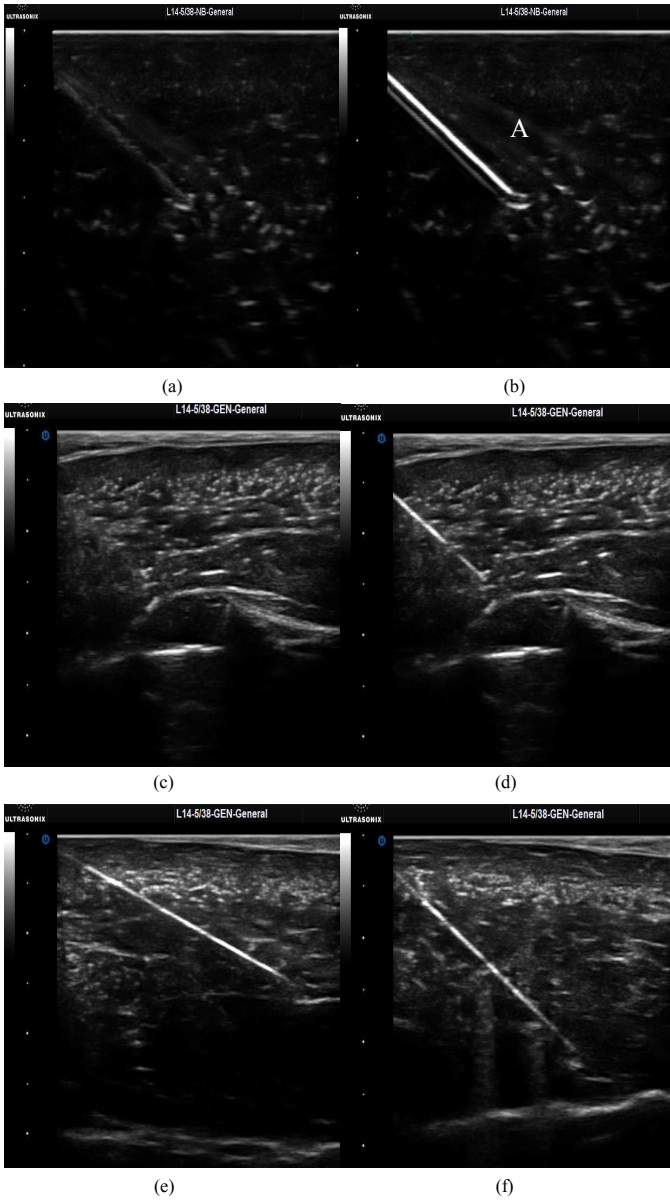


Fig. 3 (a) The phantom image using the normal spatial compounding. (b) The phantom image using the proposed adaptive spatial compounding. (c) The chicken image using the normal spatial compounding. (d) The chicken image using the proposed adaptive spatial compounding. (e) The chicken image using the proposed adaptive spatial compounding with shallow insertion angle ( $\sim 20$  degree). (f) The chicken image using the proposed adaptive spatial compounding with deep insertion angle ( $\sim 50$  degree).

the needle in multiple directions, e.g. 20, and 50 degrees without changing any ultrasound parameters. The effect of needle enhancement for each needle insertion angle will be evaluated.

### III. RESULT

Fig. 3 (a) and (b) show the difference between the normal spatial compounding and the proposed method in phantom. The needle image is seen much clearer in the proposed result. In this example, the  $m$  factor in the proposed method was set to 8. The higher the  $m$  factor, the brighter the needle image until it saturates. This results in a strongly enhanced needle echo. The CNR of the needle is therefore has been improved from 5.23 to 54. The reason we set the  $m$  factor this high is there would be a lot more attenuation in tissue. As shown in Fig. 3(d), the enhanced needle is weaker with the same  $m$  setting in the chicken breast compared with in the phantom. However, without

the proposed approach, the needle is almost disappeared in the Fig. 3(c). The needle CNR is changed from 0.78 to 4.58 from Fig. 3(c) to Fig. 3(d). We can also clearly see that there is not any significant noise added in the result image other than needle, therefore not affecting the image quality. As a comparison, we can see some line artifact is introduced in the phantom scenario (region A in the Fig. 3(b)). This artifact is generated by the side lobe of the ultrasound beam. We will discuss about it in detail in the discussion section and provide methods to remove it.

Fig. 3(e) and (f) show the needle can be enhanced inside the chicken both with a shallow insertion angle ( $\sim 20$  degree) and a deep insertion angle ( $\sim 50$  degree) without any parameter adjustments. This is promising since it may be hard for the users to estimate the needle insertion angle prior to the insertion. Meanwhile, it's pretty common that users would adjust their needle inside the body to multiple different paths to access different parts of the target. Our method would guarantee the enhancement of the needles for most common directions.

We have also evaluated the processing speed of the proposed method. For a regular NE frame of  $64 \times 512$  pixels, the processing time of the tensor-based filter is less than 4 ms. The overall processing time which includes scan conversion and merging is less than 12 ms. This fast implementation ensures no significant frame rate drop for the proposed method.

### IV. DISCUSSION

The proposed adaptive spatial compounding method offers high needle/tissue CNR. The noise from tissue in the NE frames can be effectively removed through the proposed dynamic range adjustments and tensor-based analysis. However, some artifacts generated from the needle directly could also be enhanced. For example, the A region in Fig. 3(b) shows the artifact coming from the side lobe of the frames that have the same steering angle as the needle insertion direction. These side lobes interact with the needle and forms lines like a fake needle. Because of the strong line structure nature, these lines will also be enhanced by the proposed tensor-based method. To remove these fake lines, we can set which side of the probe the needle will be inserted in. Then we only steer images towards that side. For example, when the needle will be inserted in the left side of the probe as shown in Fig. 3, the NE frames would only have steering angles of  $-45$ ,  $-30$ , and  $-15$  degrees. In this case, the needle can be enhanced without fake lines with a trade-off on flexibility. Another potential method to remove the artifact would be reducing the receive aperture. The problem of this approach is the true needle echo could also be weakened. Since the needle artifact generated by the side lobe is usually weaker than the actual needle, which means the major Eigen values are smaller, we can put a threshold in the Major Eigen values. Only pixels with Eigen values larger than that threshold will be enhanced. This Eigen value thresholding can also limit the false enhancement of the tissue layers that have the same direction as the needle insertion direction.

Calculating the directional filters in all four directions could be computationally expensive. We can significantly reduce the amount of computation by knowing the needle should be inserted in a direction that is perpendicular to the ultrasound beam. Only one instead of four high pass filters can be used which only enhances lines along that direction. Other lines, such as the lines created by the side lobe, which is not perpendicular to the ultrasound beam won't be enhanced. The computation can be reduced while at the same time we can reduce the artifact along other directions.

Due to the line structure nature of the needle, line detection algorithms, such as Hough transform, could also be used to detect and enhance the needle. The benefit for using the line detection would be able to connect the broken needles as shown in Fig. 3(d).

However, the use of line detection algorithm requires the needle has been advanced for a relatively long distance inside the body. This means no needle can be enhanced when it's just entering the image. Meanwhile, the needle tip position is hard to estimate in the line detection algorithms. Due to these drawbacks, we don't recommend using the line detection algorithms in the needle enhancement.

Similar as most needle enhancement methods, the proposed algorithm can only enhance the needle visualization when it's inside the ultrasound imaging plane. However, in many cases, the needle needs to be inserted out-of the imaging plane due to the geometry limitations. In this scenario, additional needle localization devices, such as SonixGPS [13-15] system, could be employed.

## V. CONCLUSION

In this paper, we have proposed an adaptive tensor-analysis based spatial compounding method to enhance the needle visualization. It can enhance the needle with a big variety of insertion angels. Phantom and *in-vitro* studies have proved that the needles can be enhanced without introducing significant artifacts. Real-time implementation of the proposed method has also been achieved. We believe the proposed method could be useful in the real-time guidance of needle insertion.

## REFERENCES

- [1] L. Rodriguez, M. Terris, "Risks and complications of transrectal ultrasound guided prostate needle biopsy: a prospective study and review of the literature", *Journal of Urology*, vol.160, pp 2115-2120, 1998.
- [2] K. Chin, A. Perlas, V. Chan, R. Brull, "Needle Visualization in Ultrasound-Guided Regional Anesthesia: Challenges and Solutions", *Reg. Anesth. Pain Med.*, vol.33, pp 532-544, 2008.
- [3] B. Sites, B. Spence, J. Gallagher, C. Wiley, M. Bertrand, and G. Blike, "Characterizing novice behavior associated with learning ultrasound-guided peripheral regional anesthesia", *Reg. Anesth. Pain Med.*, vol.32, pp 107-115, 2007.
- [4] P. Phal, D. Brooks, and R. Wolfe, "Sonographically guided biopsy of focal lesions: A comparison of freehand and probe-guided techniques using a phantom", *AJR Am J Roentgenol*, vol. 184, pp 1652-1656, 2005.
- [5] T. Matalon and B. Silver, "US guidance of interventional procedures", *Radiology*, vol. 174, pp. 43-47, 1990.
- [6] T. Maecken, M. Zenz, and T. Grau, "Ultrasound characteristics of needles for regional anesthesia", *Reg. Anesth. Pain Med.*, vol. 32, pp 440-447, 2007.
- [7] M. Phelan, C. Emerman, and W. Peacock, "Do echo-enhanced needles improve time to cannulate in a model of short axis ultrasound-guided vascular access for a group of mostly inexperienced ultrasound users?", *Int. J. Emerg. Med.*, vol. 2, pp 167-170, 2009.
- [8] J. Takatani, N. Takeshima, K. Okuda, Y. Oyama, T. Uchino, and T. Noguchi, "New ultrasound software delineates the needle brightly even at the angle of 60 degrees", *European Journal of Anesthesiology*, vol. 28, pp 42, 2011.
- [9] H. Knutsson, L. Haglund, H. Barman, G.H. Granlund, "A framework for anisotropic adaptive filtering and analysis of image sequences and volumes," *Acoustics, Speech, and Signal Processing*, vol. 3, pp.469-472, 1992.
- [10] M. Cohnen, A. Saleh, R. Lüthen, J. Bode, and U. Mödder, "Improvement of sonographic needle visibility in cirrhotic livers during transjugular intrahepatic portosystemic shunt procedures with use of real-time compound imaging," *J Vasc Interv Radiol*, vol. 14, pp 103-106, 2003.
- [11] M. Andersson, and H. Knutsson, "Transformation of local spatio-temporal structure tensor fields", *IEEE Proceedings of Acoustics, Speech, and Signal Processing*, vol.3, pp 285-288, 2003.
- [12] G. Farnebäck, "Polynomial expansion for orientation and motion estimation", *Ph.D. thesis*, Linköping University, Sweden, 2002.
- [13] L. Pelissier, B. Zhuang, K. Dickie, C. Leung, "Ultrasound systems incorporating spatial position sensors and associated methods", *US patent application 20100298712*, 2010.
- [14] L. Pelissier, B. Zhuang, K. Dickie, C. Leung, "Freehand ultrasound imaging systems and methods for guiding fine elongate instruments", *US patent application 20100298705*, 2010.
- [15] L. Pelissier, B. Zhuang, K. Dickie, C. Leung, "Freehand ultrasound imaging systems and methods providing position quality feedback", *US patent application 20100298704*, 2010.